

ChemComm

Accepted Manuscript



This is an *Accepted Manuscript*, which has been through the Royal Society of Chemistry peer review process and has been accepted for publication.

Accepted Manuscripts are published online shortly after acceptance, before technical editing, formatting and proof reading. Using this free service, authors can make their results available to the community, in citable form, before we publish the edited article. We will replace this *Accepted Manuscript* with the edited and formatted *Advance Article* as soon as it is available.

You can find more information about *Accepted Manuscripts* in the [Information for Authors](#).

Please note that technical editing may introduce minor changes to the text and/or graphics, which may alter content. The journal's standard [Terms & Conditions](#) and the [Ethical guidelines](#) still apply. In no event shall the Royal Society of Chemistry be held responsible for any errors or omissions in this *Accepted Manuscript* or any consequences arising from the use of any information it contains.



ChemComm

COMMUNICATION

Flexible Perovskite Solar Cells Based on Metal-Insulator-Semiconductor Structure

Received 00th January 20xx,
Accepted 00th January 20xx

Jing Wei,^{a,b} Heng Li,^{a,b} Yicheng Zhao,^{a,b} Wenke Zhou,^{a,b} Rui Fu,^{a,b} Huiyue Pan^c and Qing Zhao^{† a,b}

DOI: 10.1039/x0xx00000x

www.rsc.org/

Metal-insulator-semiconductor (MIS) structure is applied into perovskite solar cells, in which traditional compact layer TiO₂ is replaced by Al₂O₃ as hole blocking material to realize all-low-temperature process. Flexible devices based on this structure are also realized with excellent flexibility, holding 85% of its initial efficiency after 100 times bending.

The recent breakthrough of perovskite solar cells (PSCs) has led to power conversion efficiencies of over 20%.¹ For their low cost, simple fabrication, and high efficiency, PSCs have emerged as the most promising new generation of photovoltaic technology.²⁻⁴ The instability,⁵ current-density-voltage (*J*-*V*) hysteresis⁶ and high temperature process⁷ remain to be solved for industrialization. Many works have been reported for the stability and hysteresis of perovskite,⁸⁻¹¹ but few focus on the high-temperature process of TiO₂ layer in n-i-p structure, which will bring in high power consumption and hinder the way to make flexible solar cells.¹² Organic structure based on PCBM/PEDOT: PSS, alternative electron transport layers like ZnO and low-temperature process for TiO₂ layer have been tried to solve the problem.¹³⁻¹⁷ However, they all inevitably introduce some new problems, like lower stability, higher cost and inferior performance.

To date, most PSCs are fabricated in the sandwiched structure: the perovskite light absorber is placed between electron-transport layer (ETL) and hole-transport layer (HTL).¹⁸⁻²⁰ Photo-generated electrons will be extracted by ETL and blocked by HTL. Since the presence of both interfaces is not a prerequisite for device function, because perovskite possesses long-range balanced electron- and hole-transport lengths,^{21, 22} a number of reports have emerged on HTL (or ETL) -free perovskite solar cells.²³⁻²⁵ ETL-free devices avoid the high temperature process of compact TiO₂, which may be a

good choice for all-low-temperature-processed PSCs. However, without hole blocking layer, this structure inevitably suffers from electric leakage at the interface of FTO and perovskite. The ETL-free structure seems to be Schottky contact, similar to the silicon-based Schottky-barrier solar cells.^{11,12} Schottky-barrier solar cells have lower power conversion efficiency (PCE) than those based on p-n junctions. In the Schottky solar cells, the metal-semiconductor interface has seriously pinning effect, which reduces the Schottky barrier, brings in higher dark current, and decreases the open-circuit voltage (*V*_{oc}).²⁶ Insulator layer is introduced to Schottky contact to increase the open circuit voltage (*V*_{oc}), short circuit current density (*J*_{sc}), and fill factor, by inhibiting dark current caused by the majority carriers, which is known as metal-insulator-semiconductor (MIS) solar cells.²⁷ This MIS solar cell can work with tunneling current.²⁸

Here we replace TiO₂ compact layer to ultra-thin insulate Al₂O₃ as hole blocking material, and fabricate perovskite solar cells with MIS structure. After optimizing the process parameters, this structure results in good efficiency (14.6%) with simple, low-temperature process. A model based on MIS structure was employed to clarify the working mechanism of the device. In addition, owing to the low temperature process for insulating layer deposition, flexible MIS-PSCs were fabricated to realize flexible energy devices with good device performance and flexibility. The flexible solar cells can hold 85% of its initial efficiency after 100 times bending.

The concept of MIS-PSCs is illustrated in Fig. 1a, with the structure of transparent conductive electrodes (FTO)/hole blocking layer (Al₂O₃)/perovskite/hole transporting layer (spiro-OMeTAD)/top electrode (Au). Fig. 1b shows the energy levels of the device components. Electrons will be transported to FTO by tunneling effect through Al₂O₃ layer, and holes will be extracted by HTL.

Different thickness of Al₂O₃ layers (0-3 nm) was deposited onto FTO glass using atomic layer deposition (ALD) method to determine the best parameters for the MIS-PSCs. Because the performance of the device lies crucially on the thickness of Al₂O₃ film, monitoring the deposition thickness precisely becomes the key to study the mechanism and get good devices. ALD method is a good choice to realize uniform and compact Al₂O₃ layer with such thin and accurate thickness. TiO₂ compact layer was also deposited by ALD previously.¹⁶ However, depositing 20 nm TiO₂ film by ALD at low

^a State Key Laboratory for Mesoscopic Physics and Electron Microscopy Laboratory, School of Physics, Peking University, Beijing 100871, China.

^b Collaborative Innovation Center of Quantum Matter, Beijing 100084, China.

^c 1585 Clifton Rd Ne Atlanta GA 30329.

[†] Corresponding author. Email address: zhaqing@pku.edu.cn

Electronic Supplementary Information (ESI) available: Experimental section for device preparation, *J*-*V* curves, photoluminescence and impedance spectrum measurement are included in supplementary information. See DOI: 10.1039/x0xx00000x

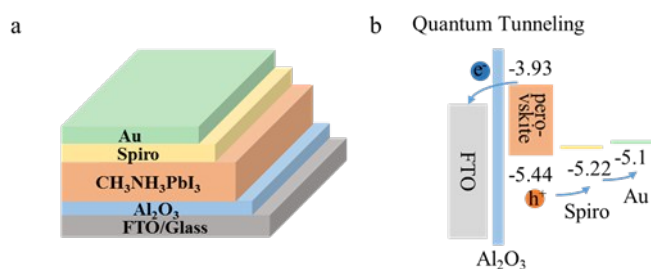


Fig. 1 Schematic representation of MIS-PSC structure (a) and the energy levels of the device components (b).

temperature below 100 °C needs about 10 hours, which is a long time for industrial manufacture. In this work, depositing Al₂O₃ layer of 1~3 nm thickness only takes minutes by ALD, showing big convenience and superiority compared to TiO₂. *J-V* curves under dark and light (100 mW/cm² AM1.5 simulated sunlight) of the corresponding devices are shown in Fig. 2a,b. *J-V* curves under dark show typical diode characteristics, implying that the shunt resistance of the devices is very large, except device with 3 nm Al₂O₃ layer, which may be too thick to achieve the tunneling current. Additionally, the threshold voltage is increasing with larger thickness of Al₂O₃, indicating more voltage falling on the Al₂O₃ layer. Larger threshold voltage may bring bigger open circuit voltage in the solar cell, but it can also decrease the current. This speculation is confirmed by the results of Fig. 2b. The device of 1 nm Al₂O₃ shows the best photovoltaic performance, while 2~3 nm Al₂O₃ reduces in turn, mainly caused by the reduction of photocurrent and fill factor. Thus we can lock the parameter of Al₂O₃ thickness at ~1 nm. After more detailed experiments for the Al₂O₃ thickness varied from 0.5 nm to 1.5 nm (Fig. 2b), we finally determine the thickness to 1.0 nm, and the device shows its best PCE of 14.6%. We further measure the photocurrent over time at a fixed voltage close to maximum power point to determine the real working status of the device. As shown in Fig. 2c, the photocurrent rises up to the maximum value almost instantly as turning on the illumination, as well as it falls as turning off the light, showing good photo response, corresponding to the good contact of interfaces and high quality of perovskite¹⁰. The PCE reaches to 13% and remains at ~12%, showing good working performance of the MIS-PSCs. Hysteresis of the *J-V* curves has also been studied and the results are shown in the supporting information (Fig. S1, 2).

To seek out the function of Al₂O₃ layer in devices, we should make clear the working mechanism of MIS structure.²⁹ As shown in Fig. 3, when Al₂O₃ is thin enough, the structure will work as a Schottky junction. This structure will bring in carrier recombination and big dark current. When thickening Al₂O₃ layer to proper thickness, photo electrons can be transported to FTO by tunneling effect. And holes will be blocked by the barrier and extracted by HTL. Further thickening the Al₂O₃ layer will hinder the electron transport due to its insulating property. From the parameters of MIS solar cells based on SiO₂ insulator³⁰, we can roughly estimate that 1~3 nm thickness may work as “tunnel” junction here, which has been confirmed by the *J-V* measurement above.

A model based on MIS solar cells was put forward to analyse the *J-V* properties of the devices, to further clarify the photovoltaic characteristics. The equivalent circuit is shown in the inset of Fig. 4a, and the *J-V* characteristic of the model is described as^{23, 31, 32}

$$J = J_L - J_0 \left[\exp\left(\frac{e(V+J \times R_s)}{A k_B T}\right) - 1 \right] - \frac{V+J \times R_s}{R_{sh}}, \quad (1)$$

where

$$J_0 = n \times T^2 \exp(-q\Phi_b/k_B T) \times \exp(-\chi_n^{1/2} \delta). \quad (2)$$

J, *J_L*, *J₀* stands for the output current density, light induced current density, and reverse saturated current density, respectively; *R_s*, *R_{sh}* represents the series resistance and shunt resistance, respectively; *A* is the ideality factor of a heterojunction, *k_B* is the Boltzmann constant, *T* is the absolute temperature, *V* is the DC bias voltage that applied at the cell, *n* is a constant, *Φ_b* is the barrier height of insulator layer, *χ_n* stands for the electron affinity, and *δ* is the thickness of the insulator layer. Assuming that *R_{sh}* is very large, from equation (1), we can deduce:

$$-\frac{dV}{dJ} = \frac{A k_B T}{e} (J_{SC} - J)^{-1} + R_s \quad (3)$$

R_s and *A* can be derived from equation (3), helping us to analyze the performance of devices. Fig. 4a gives the plots of *dV/dJ* versus (*J_{SC}* - *J*)⁻¹ with the linear fitting curves according to equation (3) based on devices of 2 nm Al₂O₃ layer. There is a good linear relationship between *dV/dJ* and (*J_{SC}* - *J*)⁻¹ both at illumination and in dark, meaning that the device is a well-behaved MIS solar cell to a certain extent³¹. The ideality factor *A* and series resistance *R_s* of the device are derived from the slope and intercept of the linear fitting results in Fig. 4a. Using this method, we calculate the values of *A* and *R_s* of all the devices, and the results are shown in Table 1. For a well-behaved heterojunction solar cell, the ideality factor is usually between 1.3~2.³³ From Table 1, the ideality factors of devices with

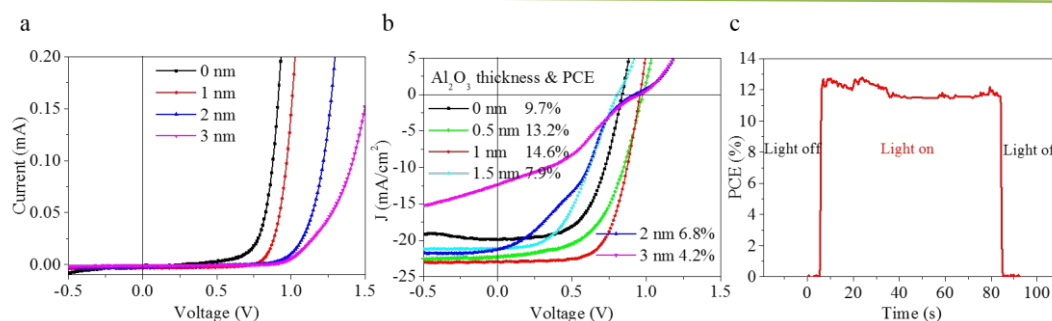


Fig. 2 Photovoltaic characterization of MIS-PSCs devices with different thickness of Al₂O₃: (a) *J-V* curves under dark, and (b) *J-V* curves under illumination, with the scanning speed of 100 mV/s; (c) Steady-state output of device with 1 nm Al₂O₃ at 0.71 V bias when light is switched on and off.

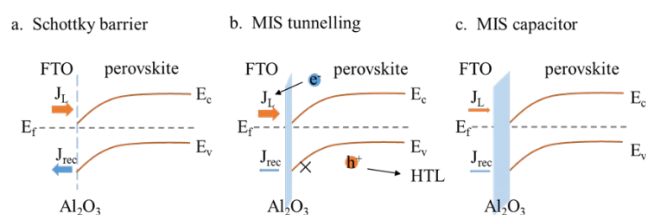


Fig. 3 Schematic energy-band diagram of the MIS-Schottky solar cells: (a) thin oxide; (b) proper oxide; (c) thick oxide.

1~3 nm Al₂O₃ layers are all between 1.3~2, both in illumination and in dark, indicating that the devices agree well with the heterojunction solar cell model. However, structure without Al₂O₃ layer shows the ideality factors of 2.24 and 2.54 in light and dark, respectively, agreeable with its poor photovoltaic performance in the solar cell. R_s increases with increasing thickness of Al₂O₃ layer, illustrating good control of Al₂O₃ thickness. For overall consideration, device with 1 nm Al₂O₃ layer shows good ideality factor and relatively low R_s , providing the best efficiency for MIS-PSCs.

Impedance spectroscopy (IS) was measured with bias from -0.2 V to 1 V. An equivalent circuit model (inset of Fig. 4b) was used to identify the main recombination process in the devices. This model is widely used to explain the Nyquist figure with only one semicircle. Constant phase element (CPE) is used for processing and analyzing the irregular semicircle impedance in Nyquist figure, and its impedance expression is

$$Z_{CPE} = \frac{R_{sh}}{1 + R_{sh}Q(j\omega)^n} \quad (4)$$

The average lifetime of carriers based on the CPE element can be derived from equation (4),

$$\tau_{avg} = (R_{sh}Q)^{1/n} \quad (5)$$

Simulating IS data based on this model, τ_{avg} extracted under various bias are shown in Fig. 4b. The result shows that the recombination rate is higher in the Schottky structure and restrained in MIS structure. The Al₂O₃ layer has two effects: decreasing the recombination and decreasing the tunnelling current. That is why 2 nm sample has larger lifetime at high bias and smaller lifetime at low bias.

Photoluminescence (PL) was measured to compare the extraction ability of MIS structure under different thickness of Al₂O₃ to photon-generated carriers. The measured MIS-films were made by spin-coating perovskite onto plasma-etched Al₂O₃/FTO glass substrate, with Al₂O₃ thickness varied from 0~3 nm. Fig. 5a shows the time-integrated PL spectra of the films. With thinner Al₂O₃ layer, photon-generated carriers were extracted quickly by the tunnelling effect, which causes big decline of spectra peaks. Time-resolved

Table 1. Ideality factors (A) and series resistance (R_s) of MIS-PSCs with different thickness of Al₂O₃ layer.

Thickness	0 nm	1 nm	2 nm	3 nm
A (light)	2.24	1.8	1.36	1.31
R_s (light)	2.37	2.45	4.39	10.02
A (dark)	2.54	1.87	1.42	1.34
R_s (dark)	2.46	3.64	6.22	10.53

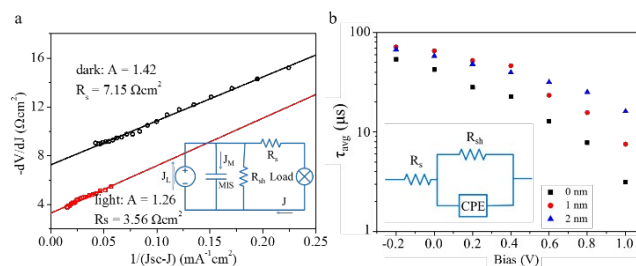


Fig. 4 Equivalent circuit of MIS-PSCs and the fitting results. (a) Plots of dV/dJ vs $(J_{sc}-J)^{-1}$ and the linear fitting curves (the inset is ideal model for MIS solar cells); (b) Impedance spectroscopy characterization of carrier recombination and the equivalent circuit model (inset). CPE stands for constant phase element.

transient PL measurements were also performed to detect the transfer of photo-generated carriers of each film. From Fig. 5b, the PL decay of films with 3 nm Al₂O₃ layer exhibits a time constant of $\tau = 85$ ns. The thinning of Al₂O₃ layer accelerates the PL decay, with observed time constants τ of 30 ns and 22 ns, for Al₂O₃ layer of 2 nm and 1 nm, respectively, showing good ability of electron transfer. The lifetime for CH₃NH₃PbI₃ film on FTO is only 7 ns, more due to its serious recombination at the interface of FTO/perovskite.

The above analysis reveal that FTO/Al₂O₃/perovskite/HTM/Au is a good MIS- heterojunction solar cell, in which perovskite/HTM act as p-n junction, where HTM has enough ability to abstract holes to Au layer; while FTO/Al₂O₃/perovskite acts as MIS structure, to restrain carrier recombination, increase V_{oc} and inhibit dark current, thus resulting in good performance of the whole solar cells. Moreover, the cell parameters, including the ideality factor and the series resistance are comparable to that of the high-efficiency thin film solar cells like Si, Cu(In,Ga)Se₂ and Cu₂ZnSn(S, Se)₄.²⁴ Since the MIS-PSCs have been demonstrated to be a good heterojunction-MIS structure like these inorganic solar cells, the mature technologies used in them could also be employed to improve the cell performance.²³

So far, we successfully fabricated solar cells based on low-temperature process, reducing the energy cost of the preparation effectively. Another advantage of this process and structure is to make flexible solar cells. In traditional PSCs, in addition to high-temperature process, the flexibility of TiO₂ layer is worse than other layers. Decreasing the thickness of this layer is a direct and effective approach to reduce the stress from bending. Replacing the 20~40 nm TiO₂ by 1 nm Al₂O₃ layer minimizes the thickness of the inorganic layer, which is a big advantage to benefit bending. As shown in Fig. 6a,b, when the film is bent, thick and compact TiO₂ film is easy to crack at surface as it

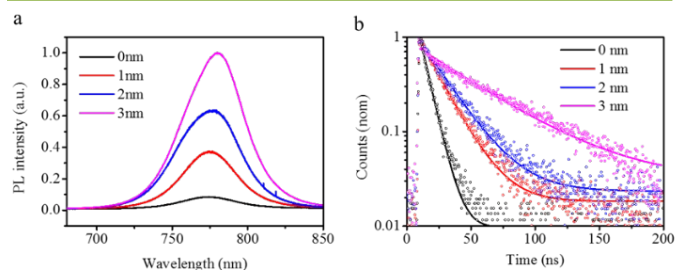


Fig. 5 PL measurement of MIS structure under different thickness of Al₂O₃. (a) Time-integrated PL spectra; (b) Time-resolved PL decay transients measured at 770±10 nm.

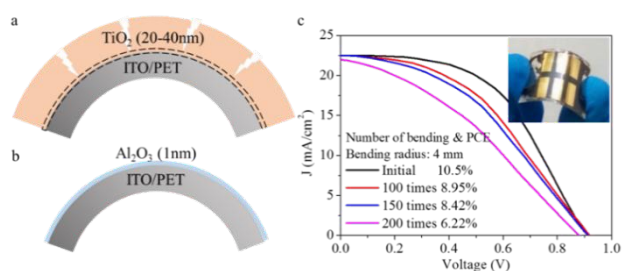


Fig. 6 (a, b) A schematic comparison of the cross section of TiO_2 layer on ITO/PET (a) and Al_2O_3 layer on ITO/PET (b) under bending. (c) Photovoltaic characterization and flexibility test of flexible MIS-PSCs with the bending radius of 4 mm (inset of c is the photo of the device).

suffers big stress; while the much thinner film of Al_2O_3 layer bears much smaller stress at the same bending radius. With this benefit, this new MIS-PSC structure performs pretty good flexibility and relatively high efficiency. Ultra-thin inorganic film greatly reduces the negative effects of bending stress on structure. From Fig. 6c, after 100, 150, even 200 times bending with the curvature radius of 4 mm, the device still holds 85%, 80% and 60% of its initial efficiency. Contrast with other flexible PSCs, which can only bear dozens of times bending,^{14, 34, 35} our MIS-PSC exhibiting much better performance of resistance flexure.

In conclusion, we proposed a new type of perovskite solar cells based on MIS structure via simple, low-temperature process. The ideal model for MIS solar cells has been applied to clarify the J - V characteristics of the devices. Some intrinsic parameters were derived, showing good MIS properties like traditional inorganic thin-film solar cells, which can provide us abundant mature technologies and experience for further development of MIS-PSCs. PL and IS measurement further verify the good carrier transfer ability of MIS structure and its well inhibitory effect on carrier recombination. Taking advantage of the low-temperature process and thinner film structure, we further make flexible solar cells on flexible substrate, getting devices with excellent flexibility and good performance. Such thin and flexible structure gives MIS-PSC unique advantage compared to traditional inorganic cells. It can be widely used in many fields, including flexible electronics, wearable power equipment, building integrated photovoltaic (BIPV), and so on, showing a large market potential and a bright future.

This work was supported by National 973 projects (2013CB932602, 2011CB707601, MOST) from Ministry of Science and Technology, China, National Natural Science Foundation of China (NSFC51272007, 61571015, 11234001, 91433102). Q.Z acknowledges Beijing Nova Program (XX2013003) and the Program for New Century Excellent Talents in University of China.

Notes and references

- W. S. Yang, J. H. Noh, N. J. Jeon, Y. C. Kim, S. Ryu, J. Seo and S. I. Seok, *Science*, 2015, **348**, 1234-1237.
- D. P. McMeekin, W. Rehman, G. E. Eperon, M. Saliba, M. T. Hörantner, A. Haghighirad, N. Sakai, L. Korte, B. Rech, M. B. Johnston, L. M. Herz and H. J. Snaith, *Science*, 2016, **351**, 5.
- W. Zhou, Y. Zhao, C. Shi, H. Huang, J. Wei, R. Fu, K. Liu, D. Yu and Q. Zhao, *J. Phys. Chem. C*, 2016, **120**, 4759-4765.
- W. Chen, Y. Wu, Y. Yue, J. Liu, W. Zhang, X. Yang, H. Chen, E. Bi, I. Ashraful, M. Grätzel and L. Han, *Science*, 2015, **350**, 5.
- Y. Zhao, J. Wei, H. Li, Y. Yan, W. Zhou, D. Yu and Q. Zhao, *Nat. Commun.*, 2016, **7**, 10228.
- J. Wei, Y. Zhao, H. Li, G. Li, J. Pan, D. Xu, Q. Zhao and D. Yu, *J. Phys. Chem. L*, 2014, **5**, 3937-3945.
- A. Mei, X. Li, L. Liu, Z. Ku, T. Liu, Y. Rong, M. Xu, M. Hu, J. Chen, Y. Yang, M. Grätzel and H. Han, *Science*, 2014, **345**, 295-298.
- T. A. Berhe, W.-N. Su, C.-H. Chen, C.-J. Pan, J.-H. Cheng, H.-M. Chen, M.-C. Tsai, L.-Y. Chen, A. A. Dubale and B.-J. Hwang, *Energy Environ. Sci.*, 2016, **9**, 323-356.
- J. You, L. Meng, T. B. Song, T. F. Guo, Y. M. Yang, W. H. Chang, Z. Hong, H. Chen, H. Zhou, Q. Chen, Y. Liu, N. De Marco and Y. Yang, *Nat. Nanotechnol.*, 2016, **11**, 75-81.
- Y. Shao, C. Bi, Y. Yuan & J. Huang, *Nat. Commun.*, 2014, **5**, 5784.
- H. J. Snaith, A. Abate, J. M. Ball, G. E. Eperon, T. Leijtens, N. K. Noel, S. D. Stranks, J. T.-W. Wang, K. Wojciechowski and W. Zhang, *J. Phys. Chem. L*, 2014.03, **5**, 1511-1515.
- J. Gong, S. B. Darling and F. You, *Energy Environ. Sci.*, 2015, **8**, 1953-1968.
- C.-C. Chen, Z. Hong, G. Li, Q. Chen, H. Zhou and Y. Yang, *J. Photon. Energy*, 2015, **5**, 057405.
- J. You, Z. Hong, Y. Yang, Q. Chen, M. Cai, T.-B. Song, C.-C. Chen, S. Lu, Y. Liu, H. Zhou and Y. Yang, *ACS NANO*, 2014, **8**, 7.
- M. M. Tavakoli, K.-H. Tsui, Q. Zhang, J. He, Y. Yao, D. Li, and Z. Fan, *ACS NANO*, 2015, **9**, 10287.
- B.-J. Kim, d. H. Kim, Y.-Y. Lee, H.-W. Shin, G. S. Han, J. S. Hong, K. Mahmood, T. Ahn, Y.-C. Joo, K. S. Hong, N.-G. Park, S. Lee and H. S. Jung, *Energy Environ. Sci.*, 2014, **7**, 94-997.
- X. Gao, J. Li, J. Baker, Y. Hou, D. Guan, J. Chen and C. Yuan, *Chem. Commun.*, 2014, **50**, 6368-6371.
- J. Wei, H. Li, Y. Zhao, W. Zhou, R. Fu, Y. L.-Wang, D. Yu and Q. Zhao, *Nano Energy*, 2016, **26**, 139-147.
- J. C. Yu, B. Kim da, G. Baek, B. R. Lee, E. D. Jung, S. Lee, J. H. Chu, D. K. Lee, K. J. Choi, S. Cho and M. H. Song, *Adv. Mater.*, 2015, **27**, 3492-3500.
- S. S. Reddy, K. Gunasekar, J. H. Heo, S. H. Im, C. S. Kim, D. H. Kim, J. H. Moon, J. Y. Lee, M. Song and S. H. Jin, *Adv. Mater.*, 2016, **28**, 686-693.
- S. D. Stranks, G. E. Eperon, G. Grancini, C. Menelaou, M. J. Alcocer, T. Leijtens, L. M. Herz, A. Petrozza and H. J. Snaith, *Science*, 2013, **342**, 341-344.
- G. Xing, N. Mathews, S. Sun, S. S. Lim, Y. M. Lam, M. Gratzel, S. Mhaisalkar and T. C. Sum, *Science*, 2013, **342**, 344-347.
- J. Shi, J. Dong, S. Lv, Y. Xu, L. Zhu, J. Xiao, X. Xu, H. Wu, D. Li, Y. Luo and Q. Meng, *Appl. Phys. Lett.*, 2014, **104**, 063901.
- W. A. Laban and L. Etgar, *Energy Environ. Sci.*, 2013, **6**, 3249.
- D. Liu, J. Yang and T. L. Kelly, *J. Am. Chem. Soc.*, 2014, **136**, 17116-17122.
- P. T. Landsberg and C. Klumpke, *Proc. R. Soc. Lond. A*, 1977, **354**, 101-118.
- D. L. Pulfrey, *IEEE T. Electron. Dev.*, 1978, **ED-25**, 1308-1317.
- S. Kar, *J. Appl. Phys.*, 1978, **49**, 5278.
- A. Banerjee, J. Yang, T. Glatfelter, K. Hoffman and S. Guha, *Appl. Phys. Lett.*, 1994, **64**, 1517.
- J. Shewchun, R. Singh and M. A. Green, *J. Appl. Phys.*, 1977, **48**, 765.
- S. S. Hegedus and W. N. Shafarman, *Comp. Mater. Sci.* 2004, **12**, 155-176.
- H. C. Card and E. S. Yang, *Appl. Phys. Lett.*, 1976, **29**, 51.
- S. M. Sze and K. K. Ng, *Physics of Semiconductor Devices*, 3rd ed. (Wiley, New York, 2006).
- C. R-Carmona, O. Malinkiewicz, A. Soriano, G. M. Espallargas, A. Garcia et al., *Energy Environ. Sci.*, 2014, **7**, 994.
- D. Liu and T. L. Kelly, *Nat. Photon.*, 2013, **8**, 133-138.